

submitted to Publications of the Astronomical Society of the
Pacific

Anisotropic Galaxy–Galaxy Lensing

Tereasa G. Brainerd & Candace Oaxaca Wright
Boston University, Department of Astronomy, Boston, MA 02215

ABSTRACT

We investigate the weak lensing shear due to dark matter galaxy halos whose mass distributions, as projected on the sky, are nearly elliptical. The shear pattern due to these halos is anisotropic about the lens centers and we quantify the level of anisotropy by comparing the mean shear experienced by sources located closest to the major axes of the lenses, $\langle\gamma\rangle_{\text{major}}$, to that experienced by sources located closest to the minor axes, $\langle\gamma\rangle_{\text{minor}}$. We demonstrate that the degree of anisotropy is independent of angular scale and show that in the case of substantially flattened halos ($\epsilon = 0.7$), the value of $\langle\gamma\rangle_{\text{minor}}$ is of order 40% of the value of $\langle\gamma\rangle_{\text{major}}$ when all sources within $\pm 45^\circ$ of the axial direction vectors of the lenses are included in the calculation. In the case of halos that are flattened at more realistic level ($\epsilon = 0.3$), the value of $\langle\gamma\rangle_{\text{minor}}$ is of order 75% of the value of $\langle\gamma\rangle_{\text{major}}$. We compute the degree to which the anisotropy in the lensing signal is degraded due to a noisy determination of the position angles of the lens galaxies and find that provided the typical $1\text{-}\sigma$ error on the orientation of the lenses is less than 15° , more than 90% of the true lensing signal will be recovered in the mean. We discuss our results in the context of detecting anisotropic galaxy–galaxy lensing in large, ground–based data sets and conclude that a modest net flattening of dark matter halos should be detectable at a statistically significant level. The forthcoming Sloan Digital Sky Survey (SDSS) data will necessarily provide a very useful data set for this analysis, but a detection of anisotropic galaxy–galaxy lensing is not dependent upon the very large sky coverage of the SDSS. Rather, we argue that a significant detection of this effect can also be obtained from an imaging survey that is of order two magnitudes fainter than SDSS and which covers only a relatively small area of sky, of order one square degree.

Subject headings: galaxies: halos — dark matter – gravitational lensing

1. Introduction

The observed flatness of the rotation curves of spiral galaxies provides convincing evidence that galaxies reside within massive dark matter halos (see, e.g., Fich & Tremaine 1991 and references therein); however, there is as yet no strong constraint on either the average radial extent or the typical shapes of these apparently pervasive structures. Since it is generally difficult to find dynamical tracers of the halo potential at very large radius, direct observational constraints on the maximum extent of dark matter halos are relatively scarce. Zaritsky & White (1994) and Zaritsky et al. (1997) have, however, investigated the dynamics of genuine satellites of bright field spirals and find that their halos extend to radii beyond $100h^{-1}$ kpc.

If the dark matter halos of bright field galaxies have radial extents that are, indeed, as large as suggested by the above investigations and the characteristic depths of the potential wells of the halos correspond to velocity dispersions of order 150 km/s, then weak but detectable gravitational lensing by the dark halos should occur. That is, systematically throughout the universe, the halos of foreground field galaxies should act as gravitational lenses for background field galaxies, resulting in a slight preference for the images of distant galaxies to be oriented tangentially with respect to the locations on the sky of galaxies which are physically closer to the observer. This effect is known as galaxy-galaxy lensing and its existence has recently been confirmed by a number of independent investigations (e.g., Brainerd, Blandford & Smail 1996, hereafter BBS; Dell’Antonio & Tyson 1996; Griffiths et al. 1996; Hudson et al. 1998; Ebbels 1998; Natarajan et al. 1998; Fischer et al. 2000). None of these studies has provided a strong constraint on the maximum physical extent of the halos of field galaxies, but all have yielded reasonably consistent measurements of the halo velocity dispersion, on the order of 150 km/s for an L^* galaxy.

Galaxy-galaxy lensing has the potential to be a powerful probe of the gravitational potential of dark halos at very large radii. It has an advantage over dynamical methods in that it can be applied to all galaxies (in particular those without genuine companions) over large physical scales, but has the disadvantage that the signal is so small that it can only be detected in a statistical sense from a large ensemble of lenses and sources. That is, while the signal is too weak to be detected from a single lens galaxy and, hence, cannot be used to place constraints on the potential of any one individual dark matter halo, it can be used to probe the mean potential of the halo population as a whole.

Because of the ability of the singular isothermal sphere model to reproduce the observed flatness of the rotation curves of the disks of spiral galaxies, it is often assumed *a priori* that dark halos are roughly spherical. However, there now exist a number of direct observations which suggest that dark halos may be substantially flattened. The evidence is

diverse, consisting of studies of the kinematics of polar ring galaxies, the geometry of X-ray isophotes, the flaring of HI gas in spirals, and the evolution of gaseous warps, as well as the kinematics of Population II stars in our own Galaxy. In particular, studies of disk systems that probe distances of order 15 kpc from the galactic planes suggest that the shapes of the dark halos are significantly flattened and can be characterized by $c/a = 0.5 \pm 0.2$ (see, e.g., the comprehensive review by Sackett 1999 and references therein). Here c/a is the ratio of the shortest to longest axis in a principal moment analysis of the mass density of the halo. More recently, Kochanek et al. (2000) have performed a detailed analysis of the shapes of the Einstein rings of three different lensed quasar host galaxies and conclude that the ellipticities of the projected mass distributions of the lens galaxies that give rise to these images are quite large indeed (axis ratios on the order of 0.6 to 0.7).

All of the published attempts to use observations of galaxy–galaxy lensing to constrain the characteristic physical parameters of dark matter halos have assumed the halos to be spherically symmetric. The lensing signal has been detected via a circular average of the signal about the lens center and is then interpreted via halo models which are spherically symmetric. However, if the halos are flattened at the level suggested by the above investigations, their projected surface mass densities will deviate from circular symmetry and, as result, the gravitational lensing pattern will not be circularly–symmetric about the lens center. Instead, the signal will be mildly anisotropic, with the shear being strongest along direction vectors that coincide with the major axis of the mass distribution and weakest along direction vectors that coincide with the minor axis of the mass distribution.

There are as yet no direct observational constraints on the mean flattening of the population of dark matter galaxy halos as a whole. This is due to the fact that the above studies which suggest substantial halo flattening rely on a handful of specific galaxies for which the particular analysis technique (e.g., dynamics, hydrodynamics, or strong lensing) may be applied. None of these techniques can be applied in general to the entire population of galaxies, but systematic galaxy–galaxy lensing can be applied to all galaxies for which high-quality imaging data is available. Despite the fact that it is only the mean 2-D shape that may be directly recovered with weak lensing (not the full 3-D shape of the halos), a strong constraint on any net flattening of galaxy halos in 2-D will be useful from the standpoint of understanding the details of galaxy formation (i.e., the interaction of baryons with the dark matter and the transfer of angular momentum to the halo as a result) and constraining the nature of the dark matter itself. In particular, dissipationless cold dark matter models routinely lead to the formation of galaxy halos with projected ellipticities of order 0.3 (e.g., Dubinski & Carlberg 1991; Warren et al. 1992), while models of strongly self-interacting cold dark matter give rise to halos that are nearly spherical within the virial radius, resulting in a small projected ellipticity (e.g., Moore et al. 2000).

Here we investigate weak lensing due to halos with elliptical mass distributions and we compare the shear experienced by sources closest to the major axes of the lenses to that experienced by sources closest to the minor axes. In §2 we describe the surface mass density profile that we have adopted, we evaluate the shear as function of location on the sky for lenses with mass ellipticities in the range $0.1 \leq \epsilon \leq 0.7$, and we compute the level of anisotropy in the galaxy–galaxy lensing signal for sources located within $\pm 45^\circ$ and $\pm 20^\circ$ of the axial direction vectors of the lenses. In §3 we discuss the prospects for detecting flattened dark halos via an anisotropy in the galaxy–galaxy lensing signal, including a consideration of some of the potential sources of noise that will be encountered in a realistic data set. A brief summary of our results is presented in §4.

2. Anisotropic Weak Shear Due to an Elliptical Lens

We adopt a surface mass density for our lenses of the form

$$\kappa(\rho) = \frac{\kappa_0}{(1 + \rho^2/x_c^2)^{1/2}} \quad (1)$$

(e.g., Schneider & Weiss 1991, hereafter SW91), which for circularly–symmetric lenses corresponds to an isothermal sphere with a core radius of x_c . Here $\kappa(\rho)$ is the surface mass density of the lens in units of the critical surface mass density (Σ_c), κ_0 is the central surface mass density, ρ is a generalized elliptical radius ($\rho^2 = x_1^2 + f^2 x_2^2$, where $f = a/b$), and the ellipticity of the mass is $\epsilon = 1 - b/a$. That is, equation (1) is an expression for the convergence of the lens and all redshift information in the problem is contained within Σ_c :

$$\Sigma_c = \frac{c^2}{4\pi G} \frac{D_s}{D_d D_{ds}}. \quad (2)$$

Here D_s is the angular diameter distance between the observer and the source, D_d is the angular diameter distance between the observer and the lens (the “deflector”), and D_{ds} is the angular diameter distance between the lens and the source.

SW91 have shown that the deflection angle, $\vec{\alpha} = (\alpha_1, \alpha_2)$, due to this mass distribution can be computed analytically and they have derived recursion relations for its computation (equations (A13) through (A19) in their paper). We have used these recursion relations to compute the deflection angles due to our elliptical masses where the ellipticities are in the range of $0.1 \leq \epsilon \leq 0.7$. Also, since the presence of a core radius does not have a significant effect on the weak lensing regime in which systematic galaxy–galaxy lensing occurs, we restrict our analysis below to the case of lenses with negligible core radii ($x_c = 0.005$ arcsec).

For each lens ellipticity, we have computed the shear due to the lens, $\vec{\gamma}(\vec{\theta}) = (\gamma_1(\vec{\theta}), \gamma_2(\vec{\theta}))$, on regular grids that were centered on the lens centers. This

was done via a straightforward differencing technique in which a regular grid of light rays was traced through each of the lenses and the net deflection of each light ray was computed from the recursion relations for $\vec{\alpha}$ contained in SW91. If $\vec{\beta}$ is the location of a given light ray on the grid prior to lensing, and $\vec{\theta}$ is the location of the light ray after having been deflected, then the components of the shear at the location $\vec{\theta}$ are simply:

$$\gamma_1(\vec{\theta}) = -\frac{1}{2} \left(\frac{\partial\beta_{x_1}}{\partial\theta_{x_1}} - \frac{\partial\beta_{x_2}}{\partial\theta_{x_2}} \right), \quad (3)$$

$$\gamma_2(\vec{\theta}) = -\frac{1}{2} \left(\frac{\partial\beta_{x_1}}{\partial\theta_{x_2}} + \frac{\partial\beta_{x_2}}{\partial\theta_{x_1}} \right). \quad (4)$$

For the calculations shown below, the spacing of the light rays on the regular grid was taken to be 0.05 arcsec.

Unlike the circular lens, for which the shear is circularly-symmetric as a function of radial distance from the lens center, the shear due to an elliptical lens is a function of both the distance from the lens center and the location of the source relative to the major and minor axes of the mass distribution of the lens (as projected on the sky). This effect is illustrated in Fig. 1, in which we plot the ratio $\langle\gamma\rangle_{\text{minor}} / \langle\gamma\rangle_{\text{major}}$ as a function of angular scale, θ . Here $\langle\gamma\rangle_{\text{major}}$ is the mean shear experienced by sources closest to the major axis direction vectors of the lens and $\langle\gamma\rangle_{\text{minor}}$ is the mean shear experienced by sources closest to the minor axis direction vectors. In the case of circularly symmetric lenses this quantity will, of course, be unity on all scales. In Fig. 1 we have computed $\langle\gamma\rangle_{\text{major}}$ and $\langle\gamma\rangle_{\text{minor}}$ for sources located within a polar angle of $\pm N$ degrees relative to the axial direction vectors of the lens, for the cases of $N = 45^\circ$ (lefthand panel), and $N = 20^\circ$ (righthand panel). That is, in the righthand panel of Fig. 1 we consider only sources whose locations on the sky are relatively close to the direction vectors defined by the major and minor axes of the mass distribution while in the lefthand panel we compute the mean shear encountered by all sources. Since all distance information is contained within κ_0 , the ratios shown in Fig. 1 are explicitly independent of the lens and source redshifts, as well as the cosmology. As expected, the degree of anisotropy in the shear pattern increases with increasing lens ellipticity, and the closer the sources are to the axial direction vectors the larger is the level of the anisotropy.

3. Prospects for Detection

Provided the ellipticity of the light from a given candidate lens galaxy is reasonably well-aligned with any flattening of its dark matter halo, it is conceivable that one could

investigate anisotropy in the galaxy–galaxy lensing signal by first aligning the symmetry axes of the lens galaxy images, then stacking the aligned images together in order to create one primary lens center about which the distortion of all the background galaxies could be measured (see, e.g., Natarajan & Refregier 2000). This will be a reasonable procedure as long as the candidate lenses are in a fairly relaxed state (i.e., one would want to exclude candidate lenses which have undergone a recent collision, for example). The detectability of the anisotropy will, of course, depend not only on the mean halo ellipticity, but also on the size of the data set (i.e., to reduce the “noise” due the intrinsic shapes of the background galaxies), the quality of the imaging data (i.e., the accuracy with which image shapes can be determined), and the success with which genuine foreground galaxies can be separated from genuine background galaxies (i.e., the ability to discriminate lenses from sources).

The mean shear due to a (spherical) singular isothermal lens within a circular aperture of angular radius θ is:

$$\bar{\gamma}(\theta) = \frac{4\pi}{\theta} \left(\frac{\sigma_v}{c} \right)^2 \left(\frac{D_{ds}}{D_s} \right). \quad (5)$$

So, for a fiducial lens with $\sigma_v = 155$ km/s, located at a redshift of $z_d = 0.5$ and a fiducial source located at a redshift of $z_s = 1.0$, the mean shear will be $\bar{\gamma}(\theta) \sim 0.30/\theta''$. (This result depends only weakly on the cosmology through the ratio of D_{ds}/D_s .) At scale of $\theta = 25''$ this is a small expected shear (of order 1%), but it is certainly measurable even with a modest-sized data set that has good imaging quality. The most statistically significant detection of galaxy–galaxy lensing to be obtained via a direct average of the observed shapes of distant galaxies is that reported by Fischer et al. (2000) from several nights of Sloan Digital Sky Survey (SDSS) commissioning data. They have detected a net shear in the images of $\sim 1.5 \times 10^6$ “faint” galaxies (r magnitudes in the range 18 to 22) due to $\sim 2.8 \times 10^4$ “bright” galaxies (r magnitudes in the range 16 to 18) over an area of nearly 225 sq. degrees and find a net shear of $\gamma \sim 0.005$ on an angular scale $\sim 30''$. On this angular scale, their detection is of order $6\text{-}\sigma$.

It is interesting to ask how large a data set would be required to obtain a significant detection of an anisotropy in the galaxy–galaxy lensing signal in the manner we have computed here. For a given surface density of lenses and sources, the signal to noise in a measurement of $\langle \gamma \rangle$ scales as the square root of the area of sky covered by the imaging data (see, e.g., BBS and Natarajan & Refregier 2000). If we compute the mean shear experienced by sources within $\pm 45^\circ$ of the major axis vectors of flattened halos, $\langle \gamma \rangle_{\text{major}}$, and compare that to the shear experienced by sources within $\pm 45^\circ$ of the minor axis vectors, $\langle \gamma \rangle_{\text{minor}}$, the signal to noise for each of these two quantities will be of order $1/\sqrt{2}$ times the signal to noise for a measurement of the mean shear experienced by all sources, as computed from a circular average about the lens centers. That is, the area over which $\langle \gamma \rangle_{\text{major}}$ or $\langle \gamma \rangle_{\text{minor}}$ is

computed is only half of the area over which the circularly-averaged shear is computed.

As a rough attempt to calculate the detectability of an anisotropy in the galaxy–galaxy signal, we will restrict ourselves to halos that have a mean flattening that is consistent with current observational constraints: $\epsilon = 0.3$ (see, e.g., Sackett 1999 or Wright & Brainerd 2000). In order to detect anisotropic galaxy–galaxy lensing at a $4\text{-}\sigma$ level from all sources within $\pm 45^\circ$ of the axial direction vectors of a halo with $\epsilon = 0.3$, we need a signal to noise in the value of $\langle \gamma \rangle_{\text{minor}} / \langle \gamma \rangle_{\text{major}}$ that is of order $(0.76/0.06) \simeq 12.7$ (see, e.g., Fig. 1, lefthand panel). By straightforward error propagation, we would then need a signal to noise in the (separate) measurements of $\langle \gamma \rangle_{\text{major}}$ and $\langle \gamma \rangle_{\text{minor}}$ on the order of 18. Assuming an identical surface density of galaxies and identical noise properties as the Fischer et al. data set, this would require an area of sky of order $[18 \times (\sqrt{2}/6)]^2 \simeq 18$ times that used by Fischer et al. (2000). That is, the amount of data required would be equivalent to about 40% of the final SDSS data set ($\sim 10^4$ square degrees). A somewhat larger survey area (of order 26 times that of the Fischer et al. data set) would be required to detect an anisotropy in $\langle \gamma \rangle_{\text{minor}}$ versus $\langle \gamma \rangle_{\text{major}}$ if one were to restrict the analysis to only those sources within $\pm 20^\circ$ of the axial direction vectors of the lenses (e.g., Fig. 1, righthand panel).

One can, of course, improve the signal to noise by using a smaller area and a data set with a completeness limit that is much greater than the relatively shallow limit of the SDSS. For example, BBS claimed a $4\text{-}\sigma$ detection of galaxy–galaxy lensing on scales $\theta \lesssim 35''$ using a single, small field (~ 72 sq. arcmin.) in which their “bright” galaxies had r magnitudes in the range of 20 to 23 and their “faint” galaxies had r magnitudes in the range 23 to 24 (i.e., roughly 2 magnitudes fainter than the SDSS data). Applying the same signal to noise calculation above to a survey with similar depth and noise properties as the BBS data, an assumption of $\epsilon \sim 0.3$ then leads to an estimate of an area of order $[18 \times (\sqrt{2}/4)]^2 = 40.5$ times that of the BBS data set (i.e., only about 0.8 square degrees) being necessary in order to obtain a significant detection of an anisotropy in the galaxy–galaxy lensing signal using sources within $\pm 45^\circ$ of the axial direction vectors of the lenses. A survey of area 1.8 square degrees would be necessary to obtain a $4\text{-}\sigma$ detection of anisotropy in the signal using sources within $\pm 20^\circ$ of the axial direction vectors of the lenses. Such relatively small areas can now be obtained easily with wide-field CCD mosaic cameras and, therefore, such an investigation is well within the reach of current technology.

There are, however, some points to note when considering the above estimation of the detectability of anisotropic galaxy–galaxy lensing. The first, and most obvious, is that both Fischer et al. (2000) and BBS separated candidate lenses from candidate sources on the basis of apparent magnitude alone. That is, since galaxies have a broad distribution in redshift, lens–source separation performed solely on the basis of apparent magnitude will

be inefficient and some of the candidate lenses are, therefore, located at greater distances from the observer than are some of the candidate sources. This will, necessarily, manifest as a source of “noise” in the analysis and will degrade the lensing signal. If lens–source separation on the basis of photometric or spectroscopic redshifts were to be performed, for example, the size of the data set that would be required to detect anisotropic galaxy–galaxy lensing would be reduced significantly from our calculation above.

Another point to note is that our estimation of the detectability of the signal is based upon an assumption of single deflections. That is, in computing the theoretical values of $\langle\gamma\rangle_{\text{minor}}/\langle\gamma\rangle_{\text{major}}$ we have not accounted for the fact that distant galaxies may be weakly lensed at comparable levels by two or more foreground galaxies. The number of multiple deflections that need to be considered depends upon the selection function used to discriminate between candidate lenses and sources, but in the case of the magnitude–selected samples of BBS it was estimated that 1/3 of the faint galaxy sample would have been lensed at a comparable level by 2 foreground galaxies, and that another 1/3 of the faint galaxy sample would have been lensed at a comparable level by 3 or more foreground galaxies. Therefore, a somewhat more reliable estimate of the detectability of anisotropic galaxy–galaxy lensing will depend upon a more detailed analysis of the problem than we have presented here. In particular, simulations of galaxy–galaxy lensing which match observational constraints as closely as possible (i.e., the faint galaxy number counts, the redshift distribution of galaxies as a function of magnitude, the luminosity function of galaxies, the range of reasonable halo shapes, and the noise properties of the data) will ultimately be required. We are in the process of completing such an analysis and will present the results soon (Wright & Brainerd 2000).

Lastly, the proposed “stacking” of the foreground galaxy images will, necessarily, be noisy at some level and this will contribute to a degradation of the anisotropic lensing signal. In particular, the effects of seeing, pixellation, and sky noise will all contribute an error to the observed position angle of the image of a foreground galaxy. In addition, galaxy–galaxy lensing of the selected foreground population due to nearby galaxies along the line of sight will contribute a small but non-zero error. That is, even in the limit of “perfect” imaging data, galaxy–galaxy lensing of the foreground population itself will cause the observed position angle of the image of a foreground galaxy to differ slightly from the true position angle of the galaxy. However, this effect is expected to be small compared to the error in the position angle that is induced by the imaging process. For example, the Monte Carlo simulations performed by BBS show that for 80% of galaxies, the position angle of the lensed image differs from that of the unlensed image by less than 5° .

In order to estimate the degree to which noise in the determination of the position

angles of the foreground galaxies results in a degradation of the anisotropic lensing signal, we repeat the calculations in §2 but with the difference that we induce an error in the observed orientation of the axial direction vectors by randomly rotating them away from their “true” location. That is, the shear experienced by the source galaxies is correctly computed as being due to flattened lenses with position angles of 0° . Then, the orientation of the axial direction vectors is randomly rotated by an amount ϕ and the mean shears, $\langle\gamma\rangle_{\text{major}}$ and $\langle\gamma\rangle_{\text{minor}}$, are computed using sources within $\pm N^\circ$ of these rotated direction vectors (i.e., the “observed” direction vectors). For simplicity of calculation, the values of ϕ were drawn from Gaussian distributions with zero mean and standard deviations of σ , where σ ranged from 5° to 45° . Computing the anisotropy in the lensing signal relative to the rotated axes will necessarily result in a value of $\langle\gamma\rangle_{\text{minor}} / \langle\gamma\rangle_{\text{major}}$ that is closer to unity than are the values plotted in Fig. 1. That is, the anisotropic lensing signal will be “degraded” by some amount, which will clearly be dependent upon the typical error in the position angles of the lens galaxies, ϕ .

By symmetry, the ratio of the mean shears is independent of angular scale (e.g., Fig. 1) for any randomly chosen value of ϕ and we therefore do not plot the angular dependence of the anisotropic lensing signal as measured relative to the rotated axes. For each value of lens ellipticity, ϵ , and standard deviation in the position angle, σ , we compute the ratio,

$$\zeta = \left[1 - \frac{\langle\gamma\rangle_{\text{minor}}}{\langle\gamma\rangle_{\text{major}}} \right]_{\text{obs}} \left[1 - \frac{\langle\gamma\rangle_{\text{minor}}}{\langle\gamma\rangle_{\text{major}}} \right]_{\text{true}}^{-1} \quad (6)$$

where the numerator is the mean value of the anisotropic lensing signal that was obtained from 5000 independent rotations of the axial direction vectors and the denominator is obtained from the values plotted in Fig. 1. That is, here we compare the relative deviations of the lensing signals from values of unity (the null case in which all halos are round in projection). The results are shown in Fig. 2, where the lefthand panel shows the degradation in the lensing signal for sources within $\pm 45^\circ$ of the rotated axial direction vectors and the righthand panel shows the same, but for sources within $\pm 20^\circ$ of the rotated axial direction vectors. The different point types refer to lenses of different ellipticities and correspond to the point types used in Fig. 1. It is clear from Fig. 2 that the anisotropic lensing signal is degraded due to the noise associated with stacking the images of the foreground lenses, but provided the typical $1\text{-}\sigma$ error in the position angle of the lenses is less than 15° , more than 90% of the true signal is recovered in the mean. The more accurate the alignment of the foreground galaxies, the more signal that will, necessarily, be recovered. Therefore, even with somewhat noisy data, anisotropies in the galaxy–galaxy lensing signal should still be detectable.

4. Summary

We have investigated anisotropies in galaxy–galaxy lensing by comparing the mean shear experienced by sources nearby to the major axis of an elliptical lens to that experienced by sources nearby to the minor axis. We have shown that for realistic halo flattening ($\epsilon \sim 0.3$), the level of anisotropy in the lensing signal is small but should be detectable in large ground-based imaging surveys. Our calculation of the size of the data set required for detection of this effect includes the actual observational error estimates in the detection of circularly-averaged galaxy-galaxy lensing from two previous investigations of galaxy–galaxy lensing: Fischer et al. (2000) and BBS. In addition, we have shown that although the level of the detected anisotropy is degraded due to noise in the process of aligning the symmetry axes of the foreground lens galaxies prior to stacking their images, the effect should be small provided the true position angles of the lens galaxies are known to within a typical $1\text{-}\sigma$ error of order 15° .

Galaxy–galaxy lensing is the only technique which at present has the potential to constrain the projected shapes of the dark matter galaxy halos on average throughout the universe. While it cannot provide a strong constraint on the shape of any one particular halo, the method is applicable to the entire galaxy population and should yield a strong constraint on the mean projected shape of halos. Given that there are currently very few observational constraints on the shapes of dark matter halos, the wealth of information on both the details of galaxy formation and the nature of the dark matter that such constraints will provide, and the apparent detectability of the lensing signal for moderately flattened halos, observational investigations of anisotropic galaxy–galaxy lensing with high-quality imaging data certainly appear to be justified at this time.

Acknowledgments

Support under NSF contract AST-9616968 and a generous allocation of resources at Boston University’s Scientific Computing and Visualization Center are gratefully acknowledged.

REFERENCES

- Brainerd, T.G., Blandford, R. D. & Smail, I., 1996, ApJ, 466, 623 (BBS)
- Dell’Antonio, I. P. & Tyson, J. A. 1996, ApJ, 473, L17
- Dubinski, J. & Carlberg, R. G. 1991, ApJ, 378, 496
- Ebbels, T. 1998, PhD Thesis, University of Cambridge
- Fich, M. & Tremaine, S. 1991, ARA&A, 29, 409
- Fischer, P. et al. (the SDSS Collaboration), 2000, AJ, submitted (astro-ph/9912119)
- Griffiths, R. E., Casertano, S., Im, M., & Ratnatunga, K. U. 1996, MNRAS, 282, P1159
- Hudson, M. J., Gwyn, S. D. J., Dahle, H., & Kaiser, N. 1998, ApJ, 503, 531
- Kochanek, C. S., Keeton, C. R., & McLeod, B. A., 2000, astro-ph/0006166
- Moore, B., Gelato, S., Jenkins, A., Pearce, F. R., & Quilis, V. 2000, astro-ph/0002308
- Natarajan, P., Kneib, J.-P., Smail, I., & Ellis, R. S, 1998, ApJ, 499, 600
- Natarajan, P. & Refregier, A. 2000, astro-ph/0003344
- Sackett, P. D. 1999, in *Galaxy Dynamics*, ASP conference series vol. 182, eds. D. R. Merritt, M. Valluri, & J. A. Sellwood, 393
- Schneider, P. & Weiss, A. 1991, A&A, 247, 269 (SW91)
- Warren, M. S., Quinn, P. J., Salmon, J. K., & Zurek, W. H. 1992, ApJ, 399, 405
- Wright, C. O. & Brainerd, T. G. 2000, in preparation
- Zaritsky, D. & White, S. D. M. 1994, ApJ, 435, 599
- Zaritsky, D., Smith, R., Frenk, C., & White, S. D. M., 1997, ApJ, 478, 39

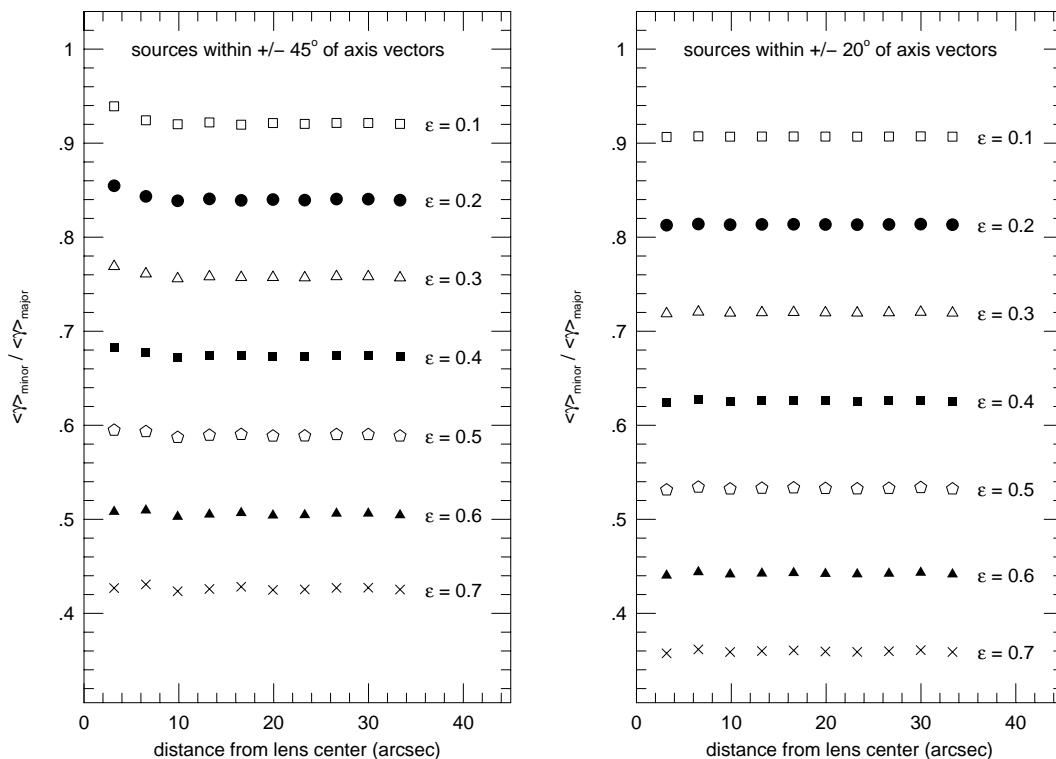


Fig. 1.— Ratio of the mean shear experienced by sources closest to the minor axis of an elliptical lens to that experienced by sources closest to the major axis of the lens. Lefthand panel: all sources that would be found within $\pm 45^\circ$ of the axial direction vectors are included in the calculation. Righthand panel: all sources that would be found within $\pm 20^\circ$ of the axial direction vectors are included in the calculation.

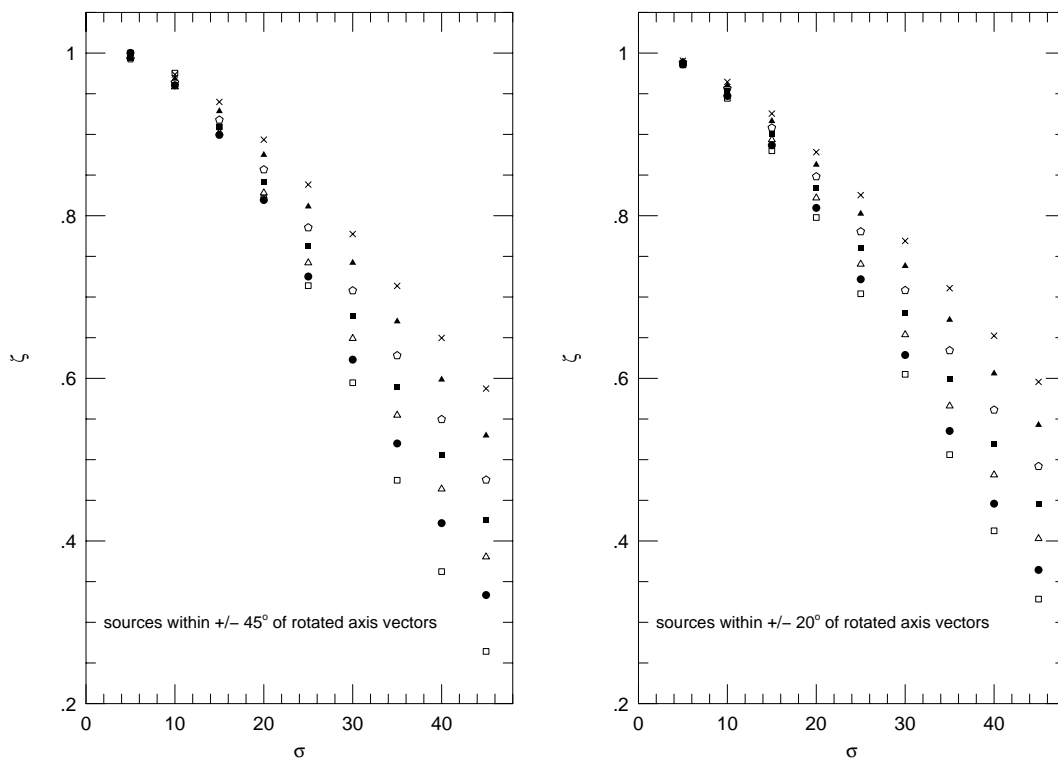


Fig. 2.— Comparison of the anisotropic lensing signal for lenses whose image position angle has been randomly rotated away from the true position angle and the lensing signal obtained without errors in the position angle (e.g., equation 6 above). The different point types indicate lenses with different ellipticities and correspond to the point types used in Fig. 1. For each value of σ , the axial direction vectors of the lens were randomly rotated 5000 times by an amount ϕ , where ϕ was drawn from a Gaussian distribution with zero mean and a standard deviation of σ . The lefthand panel shows the result for sources within $\pm 45^\circ$ of the rotated axial direction vectors; the righthand panel shows the same, but for sources within $\pm 20^\circ$.